

# Valence Electron Momentum Distributions of Ethylene from the (e,2e) Experiment

M. A. Coplan,<sup>1a</sup> A. L. Migdall,<sup>1a</sup> J. H. Moore,\*<sup>1b</sup> and J. A. Tossell<sup>1b</sup>

Contribution from the Institute for Physical Sciences and Technology and the Chemistry Department, University of Maryland, College Park, Maryland 20742.

Received February 1, 1978

**Abstract:** The momentum distributions and binding energies of the valence electrons of ethylene have been determined by electron impact ionization with complete determination of the kinematics of the incident, scattered, and knocked-out electrons. Under the conditions of high incident energy and large momentum transfer, the momentum distributions correspond to the square of the single electron momentum space wave functions. The results permit an unambiguous assignment of all the valence electrons and are compared with theoretical predictions. The shake-up state responsible for the 27.4-eV satellite in the binding energy spectrum has been identified and is shown to be principally derived from the primary state of  $^2A_g$  symmetry.

## Introduction

Most modern theoretical descriptions of the properties of large molecules employ many-electron wave functions which are approximated as antisymmetrized products of one-electron wave functions, or orbitals. These orbitals in turn are generally expressed as linear combinations of Slater or Gaussian type functions centered on the constituent atoms. Tests of the accuracy of this description generally rely on comparisons between measured and calculated one-electron properties such as orbital binding energies, transition probabilities, dipole moments, and polarizabilities. Since each of these properties is sensitive to a different spatial portion of the wave function, a meaningful comparison of theory and experiment is often difficult to achieve. In this paper we describe an experiment which not only measures one-electron orbital binding energies for the valence electrons of molecules, but yields in a straightforward way the square of the one-electron wave function in momentum space. The experiment has been applied to the simplest molecule with a carbon-carbon double bond, ethylene, for which a number of accurate theoretical wave functions exist.<sup>2,3</sup>

The experiment is called (e,2e) by analogy with the (p,2p) and ( $\alpha$ ,2 $\alpha$ ) experiments of nuclear physics from which it is derived. It is high-energy electron impact ionization with complete determination of the momenta of the incident and outgoing electrons. From conservation of momentum considerations, the momentum of the target electron before ionization is calculated. By performing the experiment many times the full momentum distribution of the target electron is determined. In addition, application of conservation of energy gives the binding energy of the knocked-out electron from the difference between the incident electron energy and the total energy of the outgoing electrons.

The quantum mechanical treatment of the (e,2e) process is based on the plane wave impulse approximation<sup>4</sup> which has been shown to be an accurate description for incident electron energies greater than ten times the binding energy of the knocked-out electron.<sup>5</sup> The quantum mechanical analogue of the classical electron momentum distribution is the absolute square of the momentum space wave function, which is in turn the Fourier transform,  $F(q)$ , of the configuration space wave function.  $|F(q)|^2 q^2 dq$  gives the probability that the electron has momentum between  $q$  and  $q + dq$ .

## Theoretical Background

SCF molecular wave functions represented by a single configuration,  $\Phi$ , can be written as an antisymmetrized product of one-electron wave functions  $\phi_i$ , in configuration space

$$\Phi = A \prod_i \phi_i$$

where  $A$  is the normalizing and antisymmetrizing operator and the product is over all occupied orbitals of the molecule. An ion created by removing an electron from orbital  $\phi_k$  can then be represented by

$$\Phi_k = A \prod_i \phi_i \phi_k^{-1}$$

Similarly, an excited state of the ion produced by the removal of an electron from  $\phi_l$  and the promotion of a second electron from  $\phi_j$  to  $\phi_\alpha$  is represented by

$$\Phi_{lj\alpha} = A \prod_i \phi_i \phi_l^{-1} \phi_j^{-1} \phi_\alpha$$

Often a single configuration wave function is not sufficient to describe an ion state. When this is the case, a configuration interaction (CI) wave function must be used. It is written

$$\Psi = \sum C_k \Phi_k + \sum_{lj\alpha} C_{lj\alpha} \Phi_{lj\alpha} \quad (1)$$

where only  $\Phi_k$ 's and  $\Phi_{lj\alpha}$ 's of the same symmetry appear. When one of the coefficients,  $C_k$ , in the first sum is much larger than any of the other coefficients, the wave function  $\Psi$  corresponds closely to the primary hole configuration  $\Phi_k$ . The energy necessary to create this configuration from the neutral ground state is equal to the negative of the energy of the  $k$ th orbital. When such a state is produced by photoionization the result is a primary peak in the photoelectron spectrum. An analogous peak would appear in the (e,2e) separation energy spectrum. More complex states are associated with nonnegligible values for several  $C_k$ 's and  $C_{lj\alpha}$ 's, but there is usually a dominant term in each sum corresponding to a particular  $\Phi_k$  and  $\Phi_{lj\alpha}$  which is used to identify the state. In both the photoelectron and (e,2e) separation energy spectra the production of such a state usually results in a satellite peak at an energy greater than that of the primary peak. The capability of the (e,2e) experiment to determine the energies of primary and satellite states and the values of the CI coefficients is one of its important features.

The cross section for the (e,2e) process is related to the wave functions for the initial and final states of the target,  $\Phi$  and  $\Psi$ , respectively. In the plane wave impulse approximation this is

$$\sigma_{(e,2e)} \propto \sigma_{e,e}(\theta) |\langle e^{i\mathbf{k}\cdot\mathbf{r}} \Psi | \Phi \rangle|^2 \quad (2)$$

where  $\sigma_{e,e}(\theta)$  is the electron-electron cross section for the scattering of the incident electron into the polar angle  $\theta$ , taking into account the indistinguishability of electrons (the Mott

cross section). The knocked-out electron has momentum  $\mathbf{k}_A$  and is represented by a plane wave  $e^{i\mathbf{k}_A \cdot \mathbf{r}}$ . Integration over the initial and final vibrational and rotational states of the molecule is implied.<sup>6</sup>

The present experiments employ the symmetric noncoplanar geometry illustrated in Figure 1. In this geometry the outgoing electrons have momenta  $\mathbf{k}_A$  and  $\mathbf{k}_B$  of identical magnitude. Their energies are  $E = (E_0 - \text{IP})/2$ , where  $E_0$  is the incident electron energy and IP is the ionization potential or separation energy of the knocked-out electron. The polar angle  $\theta$  which gives the direction of an outgoing electron with respect to the incident direction is the same for both outgoing electrons. To maximize momentum transfer to the target electron,  $\theta$  is fixed at  $45^\circ$ . The azimuthal angle  $\phi$  is the angle between the momentum vector of one of the outgoing electrons and the plane defined by the momenta of the incident electron and the other outgoing electron. By conservation of momentum, this azimuthal angle is related to the magnitude of  $\mathbf{q}$ , the recoil momentum of the target, which in the binary encounter approximation equals the initial momentum of the knocked-out electron

$$|\mathbf{q}| = \left[ (2|\mathbf{k}_A| \cos \theta - |\mathbf{k}_0|)^2 + \left( 2|\mathbf{k}_A| \sin \theta \sin \frac{\phi}{2} \right)^2 \right]^{1/2}$$

where  $\mathbf{k}_0$  is the momentum of the incident electron.

With  $\theta$  fixed,  $\sigma_{e,e}(\theta)$  is constant, and in the simple case where the ejection of an electron from the target results in a single configuration state, the relative cross section becomes

$$\sigma_k = |\langle e^{i\mathbf{k}_A \cdot \mathbf{r}} \Phi_k | \Phi \rangle|^2 \quad (3)$$

If the passive orbitals of the neutral system and the ion, those not involved in excitation or ionization, are assumed to be the same (frozen core approximation), this expression can be simplified by taking into account the orthogonality of the single electron wave functions. The result is

$$\sigma_k = |\langle e^{i\mathbf{k}_A \cdot \mathbf{r}} | \phi_k \rangle|^2$$

The integral is the Fourier transform of  $\phi_k$ , which is the single electron wave function in momentum space,  $F_k(q)$ . It follows that  $|F_k(q)|^2$  is the momentum distribution function for the knocked-out electron. The measurement of the relative (e,2e) cross section is thus sufficient to determine directly single electron wave function amplitudes; furthermore, normalization requires that

$$\int_0^\infty |F_k(q)|^2 q^2 dq = 1 \quad (4)$$

For single configuration ion states the relative (e,2e) cross sections can be put on an absolute scale by requiring

$$\int_0^\infty \sigma_k q^2 dq = 1$$

Under these conditions the relative cross sections correspond directly to probability densities.

As implied in the above treatment, the use of CI wave functions is generally confined to the representation of final ion states. Consider the common case where the initial neutral molecule state is represented by a single configuration wave function  $\Phi$  and the final ion state by two CI wave functions corresponding to the primary and satellite peaks. This situation occurs when there is only a single excited configuration of the same symmetry as the primary configuration. The CI wave functions can be written

$$\Psi^i = C^i_k \Phi_k + C^i_{lj\alpha} \Phi_{lj\alpha} \quad (5)$$

where  $i = 1$  corresponds to the primary configuration and  $i = 2$  corresponds to that of the satellite. The (e,2e) cross section

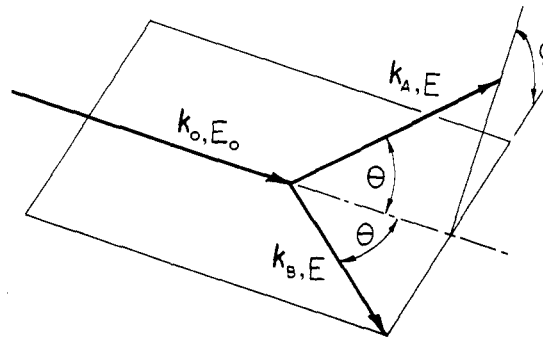


Figure 1. The symmetric noncoplanar geometry for the (e,2e) experiment.

becomes

$$\sigma^i = |C^i_k \langle e^{i\mathbf{k}_A \cdot \mathbf{r}} \Phi_k | \Phi \rangle + C^i_{lj\alpha} \langle e^{i\mathbf{k}_A \cdot \mathbf{r}} \Phi_{lj\alpha} | \Phi \rangle|^2 \quad (6)$$

where the first integral is identical with that for the single configuration case of eq 3. Again assuming that the passive orbitals are the same in the neutral molecule and the ion, the second integral reduces to two terms each of which is a product of integrals over the coordinates of the ejected and excited electron separately.

$$\sigma^i = |C^i_k \langle e^{i\mathbf{k}_A \cdot \mathbf{r}} | \phi_k \rangle + C^i_{lj\alpha} \langle e^{i\mathbf{k}_A \cdot \mathbf{r}} | \phi_l \rangle \langle \phi_\alpha | \phi_j \rangle + C^i_{lj\alpha} \langle e^{i\mathbf{k}_A \cdot \mathbf{r}} | \phi_j \rangle \langle \phi_\alpha | \phi_l \rangle|^2 \quad (7)$$

In this equation  $\phi_\alpha$  and  $\phi_j$ ,  $\phi_l$  are not orthogonal since they are eigenfunctions of the different Hamiltonians of the ion and the neutral molecule. However, the overlap integrals  $\langle \phi_\alpha | \phi_j \rangle$  and  $\langle \phi_\alpha | \phi_l \rangle$  will generally be small since even the active orbitals of the ion will be similar to those for the neutral molecule. Under this condition the first term will dominate and the variation of the (e,2e) cross section with  $q$  will be the same as that of the primary hole configuration,  $\Phi_k$ . In addition, the amplitude of the satellite state will be equal to the square of the corresponding CI coefficient. Since both the primary hole state  $\Psi^1$  and the satellite state  $\Psi^2$  correspond to the knockout of the same electron, the amplitudes of the two states sum to one. The measurement of the variation of the (e,2e) cross section with  $q$  therefore provides an unambiguous means for assigning satellite states; the amplitude of the satellite yields the CI coefficient directly.

## Experimental Results

The apparatus is a multiple detector device which is described in detail elsewhere.<sup>7</sup> For the present experiments, eight detectors were employed allowing 15 (e,2e) coincidence measurements to be made simultaneously. This arrangement permitted the experiment to be performed at a relatively high data rate with approximately three times better angular resolution than has been possible with conventional two-detector systems.

Initially, the binding energies or separation energies of the valence electrons of ethylene were determined. This is accomplished by measuring the sum of the coincidence rates in all channels as a function of scattered electron energy. Figure 2 shows the separation energy spectrum for 400-eV incident electrons. Data were accumulated for about 0.5 h at each point. This gives only moderate signal to noise ratios but since both the He I and x-ray photoelectron spectra of ethylene are available it was deemed unnecessary to accumulate data for a longer period. It is evident that all features of the photoelectron spectra appear in the (e,2e) separation energy spectrum. In particular, it should be noted that, in addition to six peaks corresponding to knockout of each type of valence electron, the well-known 27.4-eV satellite peak appears in the separation energy spectrum.

The analyzer was then set to transmit scattered electrons with energies corresponding in turn to each peak in the separation energy spectrum and the angular distribution for the knockout of each valence electron was measured. These results are presented in Figures 3 and

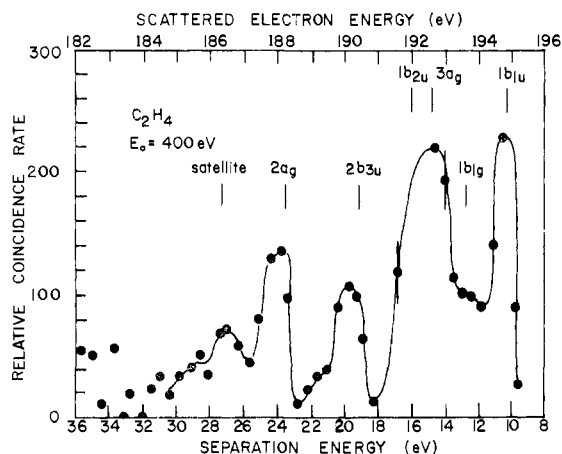


**Figure 2.** The separation energy spectrum of ethylene for 400-eV incident electrons. The vertical scale gives the sum of the coincidence rate at all azimuthal angles. The ionization potentials of the valence electrons are indicated.

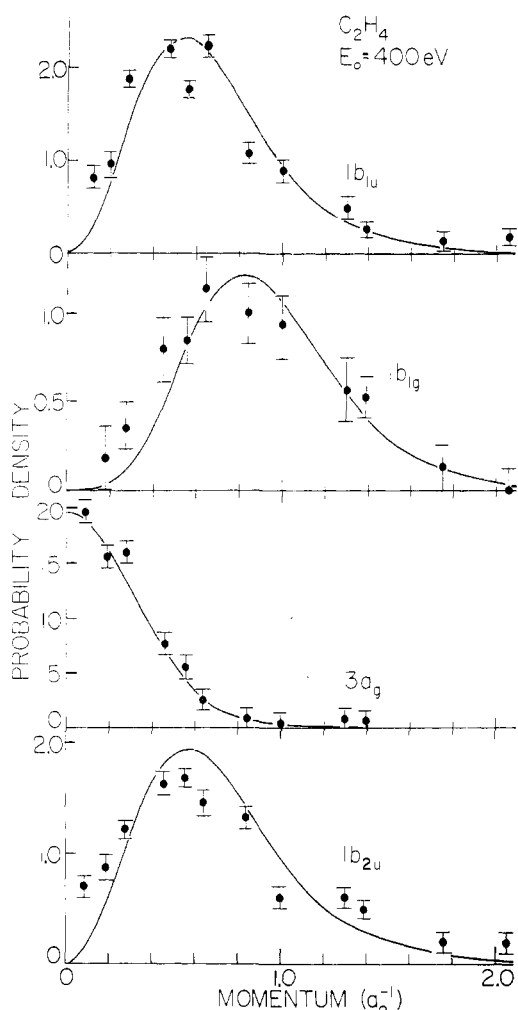


**Figure 3.** Momentum probability densities for the  $1b_{1u}$ ,  $1b_{1g}$ ,  $3a_g$ , and  $1b_{2u}$  electrons of ethylene. The experimental points are from the 400-eV, symmetric, noncoplanar, (e,2e) processes. The curves are based on the wave functions of Snyder and Basch (ref 3).

4. For comparison with the experimental results the squares of theoretical momentum space wave functions are included. The theoretical momentum distributions shown in Figures 4 and 5 were obtained by taking the Fourier transforms of the molecular orbital wave functions of Snyder and Basch.<sup>3</sup> The Snyder and Basch wave functions were obtained using the ab initio Hartree-Fock-Roothaan method, with

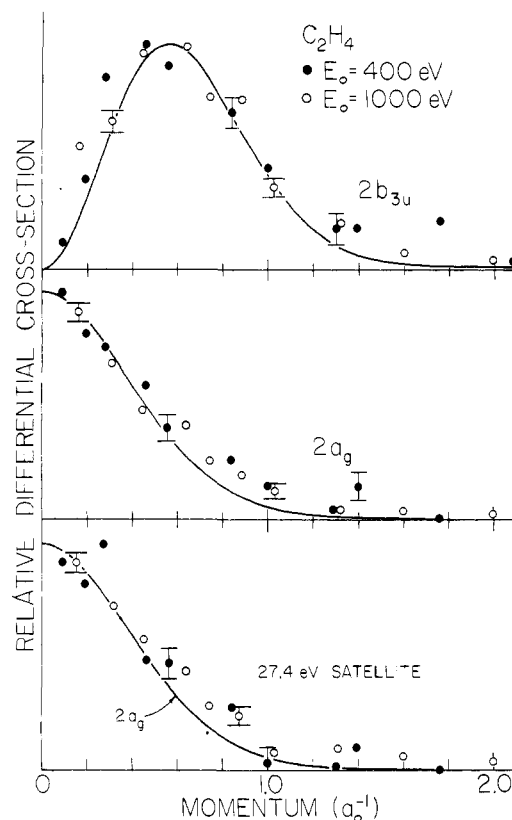


**Figure 4.** Momentum distributions for the  $2b_{3u}$  and  $2a_g$  states and the 27.4-eV satellite state of ethylene. The experimental data are from the 400- (solid circles) and 1000-eV (open circles) (e,2e) process. The curves for the  $2b_{3u}$  and  $2a_g$  are theoretical momentum distributions based on the wave functions of Snyder and Basch (ref 3). The curve shown for the satellite is identical with that for the  $2a_g$  state.

each MO being expanded in a double  $\zeta$  basis set of contracted Gaussian orbitals. Under the assumption that knockout of the  $1b_{1u}$ ,  $1b_{1g}$ ,  $3a_g$ , and  $1b_{2u}$  electrons does not result in significant population of satellite states, the momentum distributions and corresponding theoretical predictions have been normalized to give probability densities.

In order to investigate the source of intensity of the 27.4-eV satellite the relative probability,  $\sum_i \sigma(q_i) q_i^2 \Delta q_i$ , has been determined for knockout of electrons in the separation energy range from 16 to 30 eV. Since there is evidence that the intensity of the (e,2e) process for relatively deep electrons may be affected by multiple scattering or absorption of the scattered electrons,<sup>5</sup> the relative intensity measurements were carried out with an incident energy of 1000 eV in order to minimize this effect. These results are presented in Figure 5.

The theoretical and experimental momentum distributions are in reasonably good agreement for all the orbitals. In particular, the  $\pi$  orbital,  $1b_{1u}$ , is accurately described. For the  $\pi$  orbital of acetylene, on the other hand, the Snyder and Basch wave functions give a considerably smaller probability of observing electrons at low momenta than is measured.<sup>8</sup> The  $\pi$  orbital momentum distribution in  $C_2H_4$  is shifted to higher momenta relative to that in  $C_2H_2$ . This suggests that in  $C_2H_4$  the  $\pi$  orbital electron density is less uniform and/or less diffuse and thus has a larger gradient in configuration space. The  $\pi$  orbital in  $C_2H_4$ , because of its more compact nature, apparently requires fewer terms than does that in  $C_2H_2$  and the Snyder and Basch wave function thus describes it adequately.

The  $1b_{1g}$  and  $1b_{2u}$  orbitals are antibonding and bonding combinations, respectively, of the in-plane  $C2p$  orbitals (with some  $H1s$  admixture). The  $1b_{1g}$  momentum distribution occurs at higher values than that of the  $1b_{2u}$  since the  $1b_{1g}$  has a nodal plane bisecting the carbon-carbon axis. The  $1b_{1g}$  wave function, more rapidly varying in configuration space, therefore has a higher momentum distribution. Such differences between the momentum distributions of antibonding and bonding orbitals have been observed previously.<sup>9</sup>

The  $2b_{3u}$  and  $2a_g$  orbitals are predominantly antibonding and bonding combinations of the  $C2s$  orbitals. Since the antibonding  $C2s$

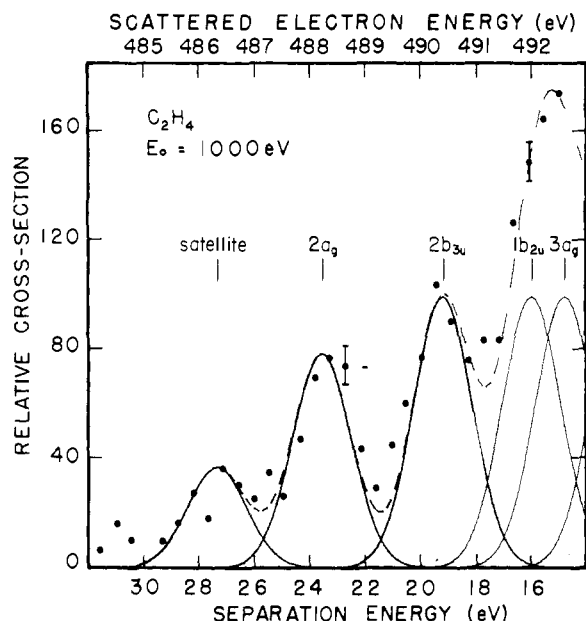


**Figure 5.** The relative cross section as a function of separation energy for knockout of an electron from ethylene in the symmetric noncoplanar (e,2e) process at an incident electron energy of 1000 eV. The instrument function is represented by solid curves centered about each ionization potential. The amplitudes have been adjusted to give the best fit (dashed line) to the experimental data.

combination in the  $2b_{3u}$  has  $p_z$  type symmetry about the center of the molecule, the momentum distribution shows a maximum not at zero but at a finite value of the momentum. For  $2s$  type orbitals we thus have qualitatively different momentum distributions for antibonding and bonding combinations.

An important feature of the (e,2e) spectrum is the satellite observed at 27.4 eV. This satellite arises from configuration interaction in the final state of the  $C_2H_4^+$  molecular ion and can be assigned using the CI wave functions of Martin and Davidson.<sup>10</sup> Their results give states at 19.2 and 23.7 eV binding energy which correspond predominantly to  $2b_{3u}$  and  $2a_g$  hole configurations of  ${}^2B_{3u}$  and  ${}^2A_g$  symmetry, respectively. (Note the reversal of  $b_{1u}$  and  $b_{3u}$  nomenclature in our work as compared to that of Martin and Davidson). The CI expansion for this lowest energy  ${}^1A_g$  state is calculated by Martin and Davidson to be  ${}^1A_g = 0.81\Phi_{2a_g} - 0.47\Phi_{2b_{3u}}^3(1b_{1u}1b_{2g}) - 0.20\Phi_{2b_{3u}}^1(1b_{1u}1b_{2g})$  where  $\Phi_{2a_g}$  is a Slater determinantal wave function with a hole in the  $2a_g$  MO and  $\Phi_{2b_{3u}}^3(1b_{1u}1b_{2g})$  has holes in the  $2b_{3u}$  and  $1b_{1u}$  orbitals and an electron in the  $1b_{2g}$ , with the  $1b_{2g}$  electron and the (remaining)  $1b_{1u}$  electron being coupled as a triplet.

There is also a state with calculated binding energy of 27.8 eV whose symmetry is also  ${}^2A_g$  and whose dominant configuration is a  $2b_{3u}$  hole coupled to a  $b_{1u} \rightarrow b_{2g}$  ( $\pi \rightarrow \pi^*$ ) excitation. The CI wave function for this second  ${}^2A_g$  state is expressed as  ${}^2A_g = 0.44\Phi_{2a_g} + 0.87\Phi_{2b_{3u}}^3(1b_{1u}1b_{2g}) - 0.15\Phi_{2b_{3u}}^1(1b_{1u}1b_{2g})$ .

The momentum distribution expected from such a CI state is given in general by eq 7 and for the specific case of the second  ${}^2A_g$  state of  $C_2H_4$  is

$$\sigma = |0.44F_{2a_g}(q) + 0.87[F_{2b_{3u}}(q)\langle 1b_{1u}(\alpha) | 1b_{2g}(\alpha) \rangle + F_{1b_{1u}}(q)\langle 2b_{3u}(\beta) | 1b_{2g}(\alpha) \rangle - 0.15[F_{2b_{3u}}(q)\langle 1b_{1u}(\alpha) | 1b_{2g}(\beta) \rangle - F_{1b_{1u}}(q)\langle 2b_{3u}(\beta) | 1b_{2g}(\beta) \rangle]|^2 \quad (8)$$

where in this case  $\alpha$  and  $\beta$  refer to the spin states of the electrons. However, in the second and third terms all the overlap integrals are equal to zero since they involve functions transforming according to different irreducible representations of the  $D_{2h}$  point group of  $C_2H_4$ . Thus, the only nonvanishing term in eq 8 involves the product of the CI coefficient of the  $2a_g$  hole state and the  $2a_g$  momentum space orbital. The satellite will then have the same momentum distribution as that of the primary  ${}^2A_g$  state at 23.6 eV, whose dominant configuration is a hole in the  $2a_g$  orbital. This result is in agreement with experiment since the momentum distribution for the 27.4-eV satellite is indistinguishable from that for the  $2a_g$  primary hole state at 23.6.

Since the only components of the CI wave functions giving nonzero contributions to the cross section are the  $\Phi_{2a_g}$  components, the intensities of the main and satellite lines may be obtained by simply squaring the coefficients of the  $\Phi_{2a_g}$  determinant within the CI wave functions. Using this procedure, Martin and Davidson calculated an intensity ratio for the 27.4-eV satellite relative to the 23.6-eV primary peak of 0.30. Mg K $\alpha$  photoelectron spectroscopy<sup>11</sup> gives a ratio of  $0.39 \pm 0.06$  while our (e,2e) result is  $0.47 \pm 0.07$ . The CI expansion performed by Martin and Davidson is of course quite limited. A larger scale CI would probably further reduce the  $2a_g^{-1}$  character in the lowest energy (main)  ${}^2A_g$  wave function thus yielding a higher ratio of first satellite to main peak intensity.

In the momentum distributions for the  ${}^2A_g$  primary and the satellite, the observed probability of finding an electron at intermediate values of momenta (from 0.6 to  $1.4 a_0^{-1}$ ) is somewhat higher than that calculated. Although this discrepancy may well be due to the difference between the Snyder and Basch SCF wave function and the exact Hartree-Fock result, it could also be due to CI in the initial state, to electronic relaxation in the ion, or to a failure of one or more of the assumptions leading to eq 7.

**Acknowledgments.** We are grateful to Professor I. R. Epstein of Brandeis University for the use of his Fourier transform program. Computer support was provided by the Computer Science Center of the University of Maryland. The Institute for Physical Science and Technology provided partial support for equipment. Thanks are also due the referees of this paper, whose comments proved most helpful. This work was supported by NSF Grant CHE76-15886-401.

## References and Notes

- (1) (a) Institute for Physical Sciences and Technology; (b) Chemistry Department.
- (2) (a) I. Fischer-Hjalmars and P. Siegbahn, *Theor. Chim. Acta*, **31**, 1 (1973); (b) S. Y. Chu, I. Ozkan, and L. Goodman, *J. Chem. Phys.*, **60**, 1268 (1974).
- (3) L. C. Snyder and H. Basch, "Molecular Wavefunctions and Properties", Wiley, New York, N.Y., 1972.
- (4) (a) I. E. McCarthy, E. V. Jezak, and A. J. Kromminga, *Nucl. Phys.*, **12**, 274 (1959); (b) Z. Mathies and V. G. Neudatchin, *Sov. Phys.-JETP (Engl. Transl.)*, **18**, 95 (1964); (c) A. E. Glassgold and G. Ialongo, *Phys. Rev.*, **175**, 151 (1968).
- (5) I. E. McCarthy and E. Weigold, *Phys. Rep.*, **27**, 275 (1976).
- (6) V. G. Levin, V. G. Neudatchin, A. V. Pavlitchenkov, and Yu. F. Smirnov, *J. Chem. Phys.*, **63**, 1541 (1975).
- (7) J. H. Moore, M. A. Coplan, T. L. Skillman, Jr., and E. D. Brooks III, *Rev. Sci. Instrum.*, **49**, 463 (1978).
- (8) (a) A. J. Dixon, I. E. McCarthy, E. Weigold, and G. R. J. Williams, *J. Electron Spectros. Relat. Phenom.*, **12**, 239 (1977); (b) M. A. Coplan, J. H. Moore, and J. A. Tossell, *J. Chem. Phys.*, **68**, 329 (1978).
- (9) I. R. Epstein and A. C. Tanner in "Compton Scattering", B. Williams, Ed., McGraw-Hill, New York, N.Y., 1977, pp 209-233.
- (10) R. L. Martin and E. R. Davidson, *Chem. Phys. Lett.*, **51**, 237 (1977).
- (11) M. S. Banna and D. A. Shirley, *J. Electron Spectrosc. Relat. Phenom.*, **8**, 255 (1976).